Cement and Concrete Composites 73 (2016) 267–280

Contents lists available at ScienceDirect

Cement and Concrete Composites

journal homepage: www.elsevier.com/locate/cemconcomp

Mechanical properties of ultra-high-performance fiber-reinforced concrete: A review

Doo-Yeol Yoo [a], Nemkumar Banthia [b, *]

[a] Department of Architectural Engineering, Hanyang University, 222 Wangsimni-ro, Seongdong-gu, Seoul 04763, Republic of Korea
[b] Department of Civil Engineering, The University of British Columbia, 6250 Applied Science Lane, Vancouver, BC V6T 1Z4, Canada

ARTICLE INFO

Article history:
Received 1 March 2016
Received in revised form
8 July 2016
Accepted 2 August 2016
Available online 3 August 2016

Keywords:
Ultra-high-performance fiber-reinforced concrete
Mechanical property
Curing condition
Steel fiber property
Size effect
Strain-rate

ABSTRACT

A comprehensive investigation into the mechanical properties of ultra-high-performance fiber-reinforced concrete (UHPFRC), considering various influential factors, is imperative in order to obtain fundamental information for its practical utilization. Therefore, this paper reviewed the early-age strength (or setting) development and mechanical properties of hardened UHPFRC. In connection with the latter, the effects of the curing conditions, coarse aggregate, mineral admixtures, fiber properties, specimen size, and strain-rate on the mechanical performance of UHPFRC were specifically investigated. It was obvious that (1) heat treatment accelerates the hydration process, leading to higher strength; (2) a portion of the silica fume can be replaced by fly ash, slag, and rice husk ash in mechanical perspective; (3) the use of deformed (hooked and twisted) or long straight steel fibers improves the mechanical properties at a static rate; and (4) high rate loading provides a noticeable increase in the mechanical properties. Alternatively, there are some disagreements between the results from various 'size effect' tests and the effectiveness of using twisted steel fibers at static and high rate loadings. Further research to reduce the production cost of UHPFRC is also addressed in an attempt to make its widespread use more practical.

1. Introduction

The mechanical properties of concrete, which fundamentally impact its practical use in construction sites, are highly dependent on numerous factors such as the type of cementitious materials, curing conditions, size of aggregates, rate of loading, specimen shape and size, etc. In particular, ultra-high-performance fiber-reinforced concrete (UHPFRC), which was developed in the mid-1990s, is very sensitive to these factors due to its extremely high compressive strength (in excess of 150 MPa) and flowable characteristics with high volume fractions of steel fibers (more than 2% by volume) [1,2]. To achieve such a high strength material, a low water-to-binder ratio (W/B) (normally W/B = 0.2) is applied with ultra-fine admixtures and heat treatment at 90 °C. As a result, the mechanical properties of UHPFRC are more significantly affected by the type of cementitious materials, curing condition, and aggregate size, as compared to those of ordinary concrete. In addition, because the mechanical properties of UHPFRC subjected to tensile and flexural loadings are strongly influenced by the fiber distribution characteristics, which are influenced by the casting process [3–5], the properties are also more sensitive to the specimen shape and size than those of ordinary concrete.

The superb compressive strength of UHPFRC leads to a significant reduction in the weight of structures made from this material; in general, the weight of structures consisting of UHPFRC is only one-third or one-half the weight of conventional RC structures under the same load [6]. Therefore, UHPFRC has attracted much attention from engineers who seek to produce more slender structures (e.g., applications in long-span bridge decks) with reducing the overall construction costs. However, slender UHPFRC structures are highly vulnerable to shrinkage cracking during the manufacturing stage because of their small cross-sectional areas and very steep increase of autogenous shrinkage at an early age. It is well-known that shrinkage cracking is influenced by both the rate/amount of shrinkage and also the strength (or setting) evolution. Therefore, the early-age strength evolution must be reviewed to precisely predict the shrinkage cracking behavior. Furthermore, knowing the early-age mechanical properties is important in order to determine the appropriate time for removal of forms and the amount of prestressing.

Typically, UHPFRC is not used in applications where ordinary

* Corresponding author.
E-mail address: banthia@civil.ubc.ca (N. Banthia).

http://dx.doi.org/10.1016/j.cemconcomp.2016.08.001
0958-9465/

concrete meets the performance criteria because of its high production cost. For this reason, achieving lower production costs is currently a key challenge for UHPFRC technology. To the best of the author's knowledge, three different methods to reduce the price of UHPFRC are currently available: (1) reducing the amount of high-strength steel fibers without deteriorating the mechanical properties (especially the tensile or flexural performance) [3,7], (2) reducing the amount of powder by using coarse aggregate [8], and (3) eliminating heat treatments or high pressure compaction [9]. These three factors clearly influence the mechanical properties of UHPFRC; thus, the effects of the steel fiber properties, coarse aggregates, and curing conditions on the mechanical properties must be addressed.

Due to its highly enhanced strength, energy absorption capacity, and unique strain-hardening behavior with multiple micro-cracks, as shown in Fig. 1, UHPFRC is considered to be a promising material for impact- or blast-resistant structures [10]. Such excellent properties can overcome the brittle nature of ordinary concrete, which often leads to an inherent poor energy absorption capacity under impact and blast loadings. The mechanical properties of concrete are influenced by the strain-rate, and the sensitivity to the strain-rate is dependent on the loading conditions and strength [11,12]. Therefore, studies involving the strain-rate effect of UHPFRC are required to be holistically reviewed.

The aim of this paper is to investigate the current state of knowledge regarding the mechanical properties of UHPFRC and to highlight some potential issues for further research. As addressed above, our attention is focused on the early-age strength (or setting) development as well as the effects of the curing conditions, coarse aggregates, mineral admixtures, fiber properties, specimen size, and loading rate on the comprehensive mechanical properties of UHPFRC.

2. Historical background of UHPFRC development

In the 1970s, the development of ultra-high-strength cement pastes with low porosity was first introduced by Yudenfreund et al. [13] and Roy et al. [14]. In Yudenfreund's study [13], a cement paste with a compressive strength of approximately 240 MPa was obtained at 25 °C after 180 days by providing a special treatment to the ground clinker with Blaine surface areas ranging from 6000 to 9000 cm^2/g and by using a low water-to-cement ratio (W/C) of 0.2. Alternatively, Roy et al. [14] obtained a cement paste with near-zero-porosity and a compressive strength of about 510 MPa by applying heat curing at 250 °C with a pressure of 50 MPa. In the early 1980s, with the development of pozzolanic admixtures and high-range water-reducing agents (i.e., superplasticizers), two different types of ultra-high-strength and low porous concretes (or pastes) were developed by Bache [15] and Birchall et al. [16] (i.e., densified with small particles (DSP) concrete and macro-defect free (MDF) pastes). DSP concrete exhibited compressive strengths ranging from 120 to 270 MPa, which were achieved by densely packing the spaces between the cement with ultra-fine particles and using an extremely low water content. Dense packing was obtained by using large quantity of superplasticizer. The concept behind MDF cement pastes was to remove macroscopic flaws during preparation; consequently, cement pastes were made with compressive strengths greater than 200 MPa and flexural strengths ranging from 60 to 70 MPa (without fiber reinforcement or high pressure compaction) [16]. Finally, in the mid-1990s, reactive powder concrete (RPC), which is the forerunner of the UHPFRCs that are currently available, was developed by Richard and Cheyrezy [17]. In their study, to achieve ultra-high strength in matrix, the size of granular materials was optimized based on packing density theory and heat (at 90 °C and 400 °C) with pressure was provided. In addition, to improve toughness of matrix, short steel fibers with a length of 13 mm and a diameter of 0.15 mm were included (1.5–3% by volume). The developed RPC exhibited compressive strengths ranging from 200 to 800 MPa and fracture energies up to 40 kJ/m^2.

3. Early-age setting and strength developments of UHPFRC

Knowing the early-age setting and mechanical strength properties of UHPFRC at any arbitrary time is important for several reasons including the removal of forms, prestressing control, and shrinkage crack control. Therefore, previous studies that investigated the early-age setting and strength development of UHPFRC are reviewed in the present study. Due to the low W/B ratio and the high fineness of the admixtures, the evaporation rate of water at exposed surfaces of UHPFRC is normally larger than that of bleeding, which causes rapid condensation of the surface even though most of the interior mortar is still fresh. This leads to plastic shrinkage cracks and durability and aesthetic problems. In particular, because of the rapid condensation of the surface, the setting evolution of UHPFRC is difficult to measure precisely. It is typically overestimated based on the penetration resistance test by ASTM C 403 [18], which is most widely used for evaluating the setting properties of fresh concrete. To overcome this problem, Yoo et al. [19] conducted several penetration resistance tests and suggested the use of paraffin oil to prevent water evaporation during the penetration resistance test. As a consequence, they obtained precise initial and final setting times for UHPFRC at 23 ± 1 °C with a relative humidity (RH) of 60± 5% of 10.8 h and 12.3 h, respectively, and the corresponding ultrasonic pulse velocities (UPVs) were determined to be 771.4 m/s and 1164.5 m/s, respectively, as shown in Fig. 2. However, the setting time varies significantly and is

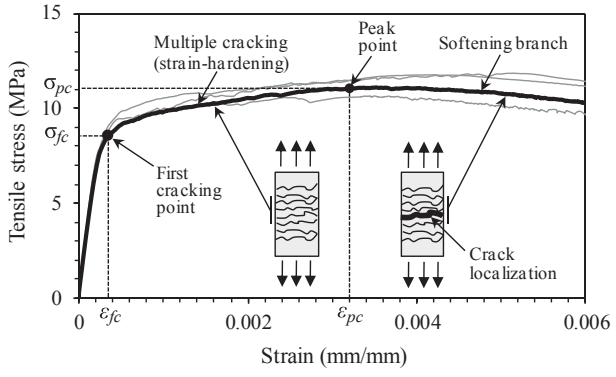

Fig. 1. Typical tensile stress versus strain behavior of UHPFRC [10].

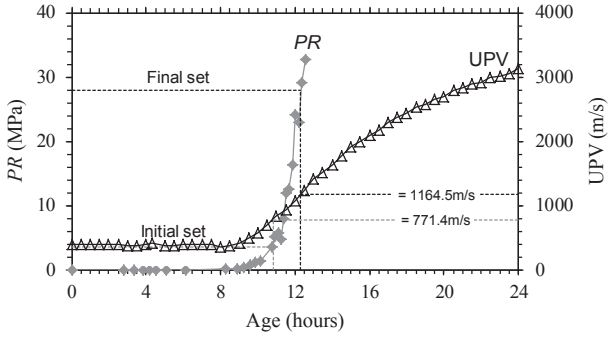

Fig. 2. Comparison of penetration resistance and UPV development [19].

dependent on the type and amount of superplasticizer, type of cementitious materials, and on whether an accelerator is included; thus, different values of initial and final setting times (15 h and 17 h, respectively) were reported by Graybeal [20]. Zhang et al. [21] estimated the setting and hardening process of UHPFRC using UPV measurements and reported several useful findings: (a) the hydration reaction is promoted by increasing the curing temperature, (b) the addition of silica fume accelerated the hydration process, whereas the use of fly ash and slag delayed the hydration process, and (c) steel fibers retard the microstructure formation process.

Based on the degree of reaction-based formulation, which is commonly used for conventional concrete, Habel et al. [22] suggested a power-type model for predicting the strength development of UHPFRC without heat treatment, as follows:

$$\frac{p(r)}{p(r=1)} = \left(\frac{r-r_0}{1-r_0}\right)^a \tag{1}$$

Here, p is the considered mechanical property, r is the degree of reaction, r_0 is the degree of reaction at the beginning of the strength development, and a is a coefficient. From their test results, the degree of reaction was found to be $r_0 = 0.16$ at approximately 32 h after the addition of water into the mixture. The degree of reaction reached 0.99 after 90 days. The coefficient was determined to be $a = 1.1$ for compressive strength, $a = 2.5$ for the first- and post-cracking tensile strengths, $a = 5$ for the tensile strain capacity, $a = 4.3$ for the fracture energy, and $a = 0.8$ for the secant modulus under compression.

Graybeal [20] performed numerous compressive tests and provided 28-day compressive strengths of 193 MPa and 126 MPa and 28-day elastic moduli of 52.7 GPa and 42.7 GPa for steam-treated and untreated UHPFRC cylinders, respectively. The Weibull Cumulative function was adopted to predict the compressive strength development of untreated UHPFRC after 0.9 days, as expressed by (Fig. 3).

$$f_{c,t}' = f_c'\left[1 - \exp\left(-\left(\frac{t-0.9}{3}\right)^{0.6}\right)\right] \tag{2}$$

Here, f_c' is the 28-day compressive strength of untreated UHPFRC and t is the age.

Graybeal [20] also proposed an equation for predicting the elastic modulus of UHPFRC at strengths above 25 MPa: $E = 3840\,(f_c')^{0.5}$.

According to the results of full-scale restrained shrinkage tests for thin UHPFRC slabs [23], shrinkage cracks occurred at a very early age (22 h and 19 h from concrete casting). However, since Eq. (1) was proposed based on test results measured approximately four days after casting, it is limited to be used for early-age shrinkage crack control. Based on the common degree of hydration model proposed by Jonasson [24], Yoo et al. [19] recently proposed the following models to predict the tensile strength and elastic modulus developments of untreated UHPFRC; these consider the very early-age tensile strength and the elastic modulus (from the initial setting time to 28 days).

$$f_t(t) = f_{t28}\exp\left\{-\lambda_1[\ln(1+(t-t_0))]^{-k_1}\right\} \tag{3}$$

$$E_t(t) = E_{t28}\exp\left\{-\lambda_2[\ln(1+(t-t_0))]^{-k_2}\right\} \tag{4}$$

Here, f_{t28} and E_{t28} are the tensile strength and elastic modulus at 28 days, respectively, t_0 is the time when the shrinkage stress first develops (time-zero), and λ_1, λ_2, k_1, and k_2 are regression coefficients. Based on the least squares error method, $\lambda_1 = 0.204$, $k_1 = 1.292$, $\lambda_2 = 0.096$, and $k_2 = 1.598$ were proposed.

Comparisons of the measured tensile strength and predicted values as a function of age for untreated UHPFRC are shown in Fig. 4. Eq. (3) satisfactorily simulated the S-shaped development of the tensile strength. Additionally, based on Eqs. (3) and (4), Yoo et al. [25] precisely estimated the early-age cracking potential and relaxed stress of UHPFRC caused by restraint of shrinkage.

4. Mechanical properties of hardened UHPFRC

As mentioned above, RPC with excellent strength and ductility was developed by Richard and Cheyrezy [17] in the mid-1990s. In order to obtain high tensile strength and ductility, 1.5–3 vol% of small-sized steel fibers (L_f of 13 mm and d_f of 0.15 mm, where L_f is the fiber length and d_f is the fiber diameter) were included. To achieve very high compressive strengths, the size of the granular mixture was optimized based on packing density theory without coarse aggregate. Pressure and heat treatment were also applied. An optimum W/B ratio between 0.11 and 0.16 was proposed based on the parameter of relative density (d_0/d_s), where d_0 is the density of concrete at demolding and d_s is the solid density of the granular mixture, which is assumed to be compact without water and air. The optimum compressive strength versus relative density for RPC with and without steel fibers and the heat treatment are shown in Fig. 5. This indicates that the compressive strength was improved by increasing the relative density, using a heat treatment, and including steel fibers. In addition, they suggested that the economic optimum fiber volume content was 2% (or about 155 kg/m^3). Based on their study, most commercially-available UHPFRC (i.e., Ductal®

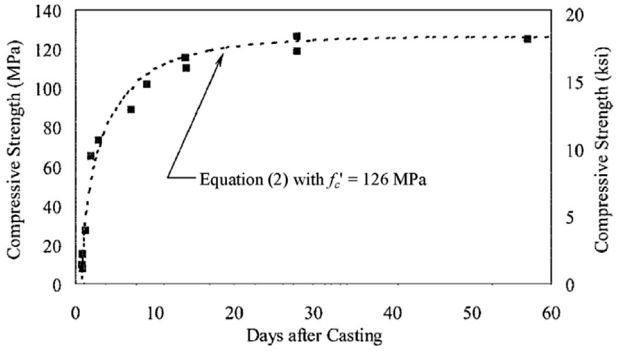

Fig. 3. Compressive strength development of untreated UHPFRC [20].

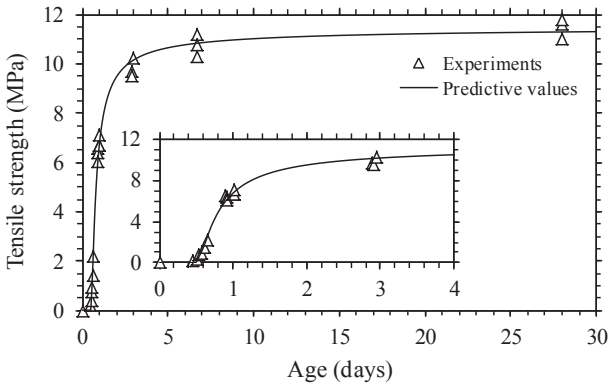

Fig. 4. Tensile strength development of untreated UHPFRC [19].

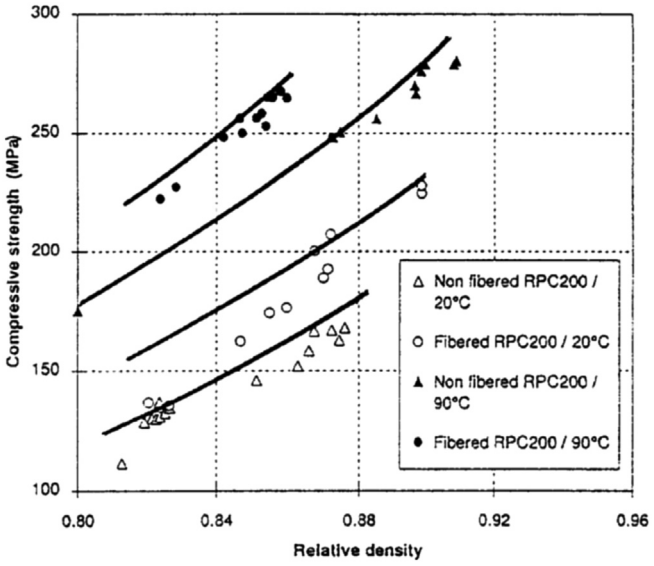

Fig. 5. Optimum compressive strength obtained from different relative densities [17].

[26], K-UHPC [27], ultra-high-strength fiber-reinforced concrete recommended by Japan Society of Civil Engineers (JSCE) [2], etc.) has a low W/B of approximately 0.2, high volume fractions of short straight steel fibers (2 vol% or more), and undergoes a heat treatment at 90 °C for 48 h or 72 h after demolding.

4.1. Effects of curing conditions

Heat treatments have generally been applied to make UHPFRC to accelerate the hydration process and increase the density, leading to ultra-high compressive strengths. In the case of precast UHPFRC products, heat curing at 90 °C for 48 h can be easily applied; thus, the target compressive strength (≥180 MPa) is generally achieved. However, in some special cases (e.g., the joints of precast segments [28] and the rehabilitation of existing structures [29]), UHPFRC is typically cast-in-place; thus, the use of heat treatments is limited due to the difficulties in controlling the temperature and moisture at a construction site. For this reason, it is important to investigate the effect of the curing conditions on the mechanical properties of UHPFRC.

Koh et al. [30] reported some useful information with regards to heat curing conditions. First, UHPFRC with wet curing at 20 °C for 91 days exhibited a similar compressive strength (approximately 200 MPa) to that of steam-treated UHPFRC at 90 °C, as shown in Fig. 6. This is consistent with the findings of Yunsheng et al. [31]. They [31] investigated the effect of curing ages on the compressive strength (curing condition: 20 °C and 100% RH) and observed an obvious increase in the compressive strength (37 MPa) from 28 days to 90 days, whereas a relatively small strength gain (8 MPa) was obtained between 90 days and 180 days. Second, UHPFRC specimens heated in a water tank at 90 °C exhibited the highest compressive strength, whereas those heated in air drying conditions at 90 °C showed the lowest compressive strength. The specimens heated with steam at 90 °C provided an intermediate value that was very slightly lower than that of the specimens heated in the water tank. Lastly, the compressive strength of UHPFRC steam-treated for 1 day was found to be approximately 155 MPa; this value increased with curing up until two days. UHPFRC steam-treated for two and three days exhibited very similar compressive strength values of approximately 195 MPa, but the strength decreased after curing for more than three days.

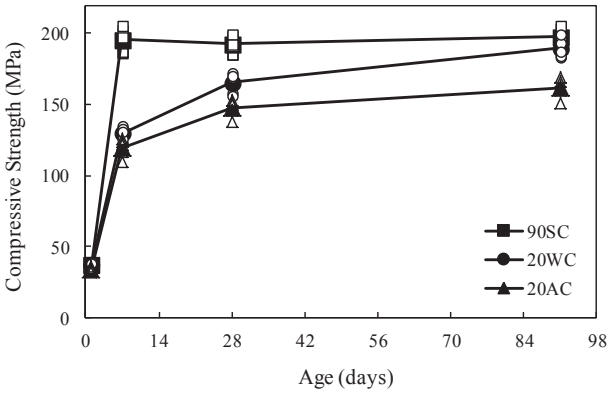

Fig. 6. Development of compressive strength of UHPFRC at with various curing conditions (90 SC = steam curing at 90 °C, 20 WC = wet curing at 20 °C, and 20 AC = air curing at 20 °C) [30].

Park et al. [32] reported that a curing time of 48–72 h is required to obtain a compressive strength of 180 MPa for UHPFRC at a curing temperature of 60 °C. A longer period of at least 96 h is required when the curing temperature is 40 °C. Ahlborn et al. [33] noted that a time delay of up to 10 or 24 days before initiating heat curing at 90 °C led to a slight decrease in the compressive strength. In addition, Soliman and Nehdi [34] reported that a higher curing temperature from 10 °C to 40 °C and a higher ambient humidity from 40% to 80% at an early age resulted in a higher compressive strength in UHPFRC. Alternatively, the addition of a shrinkage-reducing admixture (SRA) and a superabsorbent polymer (SAP) decreased the early-age compressive strength. The compressive strength was insignificantly affected by changing the W/B ratio from 0.22 to 0.25 (i.e., the difference was below 5%).

The interfacial bond strength between the fiber and matrix was significantly affected by the curing process [31]. The highest interfacial bond strength (14.2 MPa) was achieved by autoclave curing at 200 °C with a pressure of 1.7 MPa. Steam-curing at 90 °C provided slightly lower bond strength than autoclave curing, whereas a substantially lower bond strength was observed for the case of water curing at 20 °C for 28 days. The flexural strength of UHPFRC cured at 20 °C only for 28 days was lower than that cured at 90 °C or 200 °C, whereas the flexural strength of UHPFRC cured at 20 °C for 90 days became similar to that cured at 90 °C or 200 °C [31].

Previous studies [35–37] have reported that the mechanical properties of UHPFRC are degraded (e.g., lower fiber pullout resistance and mechanical strengths) when SRAs are included during heat curing. Yoo et al. [35] explained the reduced mechanical properties, especially when samples are subjected to tensile or flexural loading, as follows: (1) the radial confinement pressure, which leads to friction bonding between the fiber and the matrix, was reduced as a result of the decreased shrinkage and (2) the inclusion of an SRA resulted in a higher porosity at the interfacial transition zone (ITZ) between the fiber and the matrix. On the other hand, it was recently reported [38] that SRAs can help improve the tensile strength of UHPFRC cured at 23 °C (without heat treatment); however, the reason for this observation is still unclear.

Wille et al. [9] proposed a simple way to achieve compressive strengths over 190 MPa at 28 days without any heat treatment or pressure by using materials that are commercially available in the U.S. market. They showed that the compressive strength is closely related to the product of (W/C) × air$^{1/3}$ and proposed an optimum sand-to-cement ratio of 1.4 when using a maximum grain size of 0.8 mm, an optimum amount of silica fume (SF) (25% of the cement by weight), an optimum high-range water reducer (HRWR)

(ranging from 1.4 to 2.4% of cement by weight), and an optimum W/C ratio (of about 0.22). Based on this mixture proportion, Wille et al. [39] also obtained a highly ductile UHPFRC without needing to apply heat treatment or pressure. By including 1.5 vol% of twisted steel fibers, their UHPFRC had a post-cracking tensile strength of 13 MPa and a strain capacity of 0.6%.

4.2. Effects of coarse aggregate and admixtures

Several studies have recently been conducted to develop a new type of UHPFRC with coarse aggregates to reduce the production cost. By using a coarse aggregate, the amount of powder can be reduced, which decreases the production cost of UHPFRC. Ma et al. [8] reported that UHPFRC with coarse aggregate could be fluidized more easily and decreased the mixing time. In addition, no distinct difference in the compressive strengths was observed according to the presence of coarse aggregates. Compressive strengths of approximately 150–165 MPa at 20 °C for 28 days and 190 MPa at 90 °C were obtained for UHPFRCs with and without coarse aggregate. This is consistent with the findings of Collepardi et al. [40], who showed that replacing fine sand (0.15–0.4 mm) with coarse aggregate of a maximum size of 8 mm had no effect on the compressive strength. On the other hand, a higher elastic modulus and lower strain capacity were found in UHPFRC with coarse aggregate [8], and a lower flexural strength was obtained by including coarse aggregate [40,41]; this was caused by the lower bond strength of the fibers. With the addition of coarse aggregate, the autogenous shrinkage was reduced by approximately 40%. Based on information from the database of the International Symposium on Ultra High Performance Concrete in 2004 and 2008, Wille et al. [9] reported that UHPFRC that included coarse aggregate with a maximum grain size ranging from 7 to 16 mm rather exhibited a slightly higher compressive strength of 178 MPa, on average, compared to its counterpart without coarse aggregate (compressive strength of 162 MPa, on average).

The bond strength and pullout energy were noticeably improved as the SF content increased up to 30% [42], as shown in Fig. 7(a). The pullout energy of the UHPFRC matrix with 30% SF was almost 100% larger than that without SF. This is caused by the fact that in the case of the matrix without SF, only longitudinal scratches were obtained in Fig. 7(b); this is due to the abrasion caused by the particles during the pullout process. Alternatively, when SF was added, the matrix adhering to the fiber in Fig. 7(c) cumulated near the fiber end and contributed to an increase in the fiber pullout resistance. Yazıcı et al. [43] reported that no loss of compressive strength was observed by replacing SF with ground granulated blast furnace slag (GGBFS) and fly ash (FA) up to 40%. Also, using GGBFS and FA tended to increase the flexural strength and toughness of UHPFRC, regardless of the curing process, as shown in Fig. 8. Van Tuan et al. [44] noted that the inclusion of rice husk ash (RHA), which is an agricultural waste product, insignificantly decreased in the compressive strength compared to UHPFRC with SF (when less than 30% RHA was used). Due to a synergic effect between SF and RHA, the combined use of 10% RHA and 10% SF exhibited the highest compressive strength (higher than other samples with 20% SF or 20% RHA or without any SF and RHA). Rougeau and Borys [45] also reported that, even though UHPFRC with SF exhibited the best mechanical performance, other ultrafine admixtures (e.g., metakaolin, pulverized FA, limestone microfiller, siliceous microfiller, and micronized phonolith) can also be used to achieve compressive strengths above 150 MPa.

4.3. Effects of fiber geometry, length, and volume content

In the late 1990s, Naaman [46] developed a new type of twisted steel fiber, referred to as "Torex fiber", as shown in Fig. 9. This fiber is made by very high-strength steel wire and designed to have a polygonal cross-sectional geometry that makes it amenable to twisting along its axis. The fundamental idea behind determining the cross-sectional geometry of the Torex fiber was based on the fiber intrinsic efficiency ratio ($FIER = \psi L_f/A_f$, where ψ is the perimeter of the fiber and A_f is the area of the fiber), which is closely related to the post-cracking strength of composites. The fibers with triangular or square shapes are 28% and 12% more effective at increasing the value of the *FIER* than a circular-shaped fiber with an identical cross-sectional area [47]. As the value of the *FIER* increased, the bonding components regarding adhesion and friction were improved, and the mechanical bond was improved by twisting the fibers. The typical fiber stress and slip curves of straight, hooked-end, and twisted steel fibers embedded in a UHPFRC matrix are shown in Fig. 10 [48]. As can be seen in the figure, Wille and Naaman [48] reported that the use of twisted (and hooked-end) steel fibers achieved a maximum fiber stress that was three times higher than that of the short straight steel fibers (d_f = 0.2 mm and L_f = 13 mm); $\sigma_{f,max}$ = 2900 MPa vs. $\sigma_{f,max}$ = 1100 MPa, respectively. Based on this improved fiber pullout capacity, the tensile strength and post-cracking strain capacity of UHPFRC were also substantially improved by using the deformed (twisted and hooked-end) steel fibers, as compared to that with the short straight steel fibers [7]. The specimens with 2 vol% of twisted steel fibers exhibited a tensile strength of 14.9 MPa and a strain capacity of 0.61%; these values are

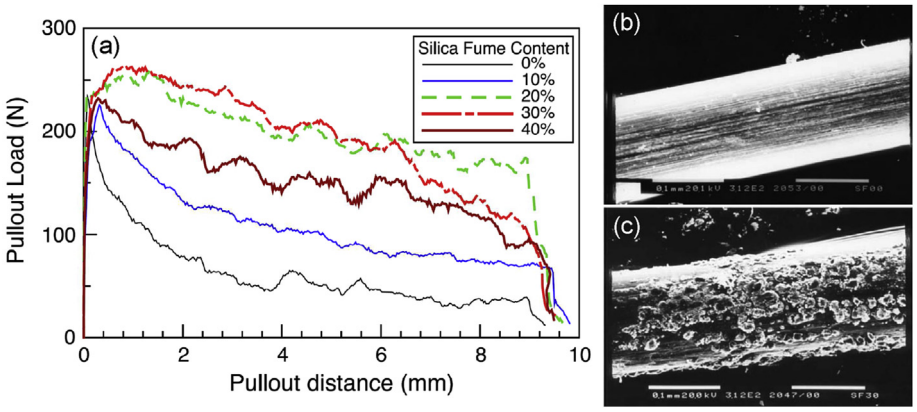

Fig. 7. Pullout behavior of straight steel fibers embedded in ultra-high-strength matrix according to SF content; (a) pullout load versus slip curve; (b) SEM observation of fiber surface (0% SF), (c) SEM observation of fiber surface (30% SF) [42].

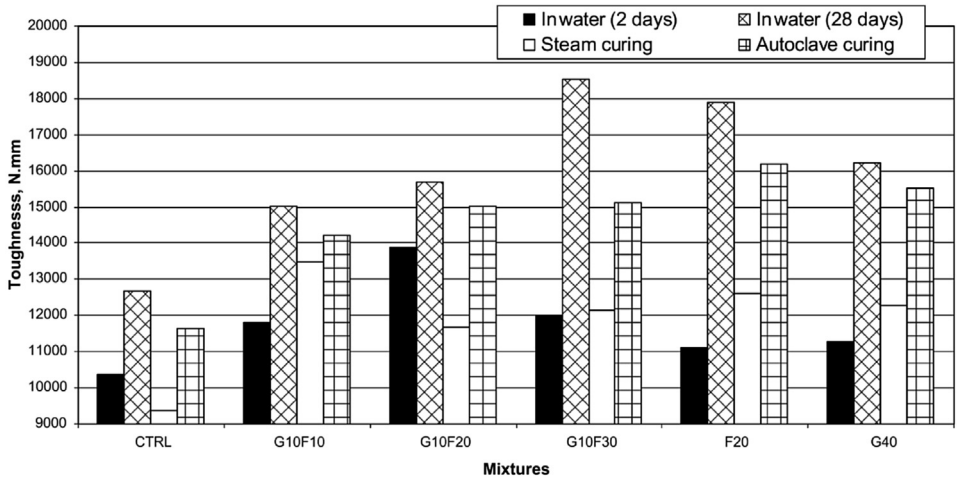

Fig. 8. Toughness of UHPFRC with various replacement ratios and curing regimes (CTRL = control UHPFRC without GGBFS and FA, G = GGBFS, F = FA, and numeral = percent of replacement) [43].

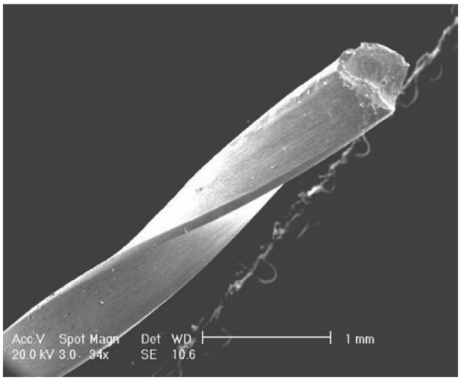

Fig. 9. Typical example of Torex twisted triangular steel fiber [47].

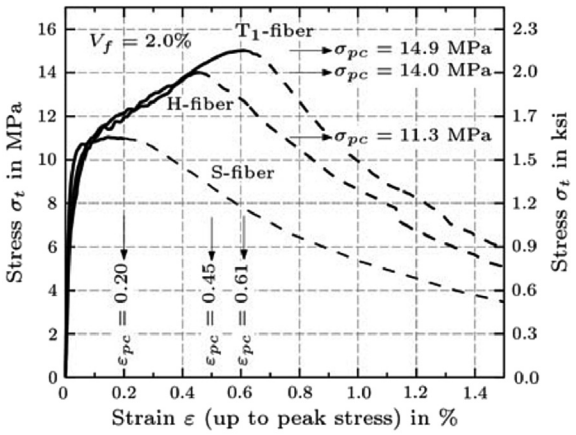

Fig. 11. Comparison of direct tensile response of UHPFRC with different types of steel fibers at V_f = 2.0% [7].

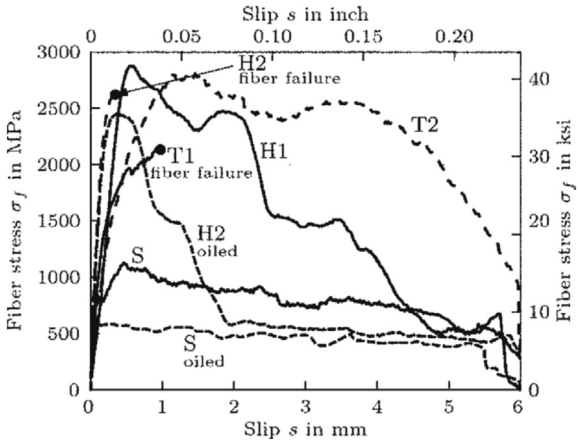

Fig. 10. Effect of fiber geometry on pullout behavior of steel fibers embedded in UHPFRC matrix (S = straight, H = hooked-end, and T = twisted) [48].

approximately 32% and 205% higher than those with 2 vol% of short straight steel fibers (Fig. 11). In addition, Yoo and Yoon [49] reported that UHPFRC beams with twisted steel fibers exhibit approximately 1.7 times higher flexural strength (f_{MOR} = 32.24 MPa) than the beams with short straight steel fibers (f_{MOR} = 19.26 MPa). The compressive behaviors, such as the compressive strength, strain capacity, and elastic modulus, were also improved by including twisted steel fibers than the use of short straight steel fibers, but the improvement was relatively insignificant compared to what was observed for the tensile and flexural performance.

Yoo et al. [3,50] recently proposed another method for improving flexural performance of UHPFRC under uniaxial and biaxial stress states and its fracture energy capacity by using long straight steel fibers. As shown in Fig. 12, the flexural strength, deflection capacity, and toughness of UHPFRC were noticeably improved by increasing the fiber length. UHPFRC panels with long straight steel fibers (L_f/d_f = 19.5/0.2 = 97.5) exhibited approximately 26% and 13% higher flexural strength and 153% and 67% higher deflection capacity than those with medium (L_f/d_f = 16.3/0.2 = 81.5) and short (L_f/d_f = 13/0.2 = 65) straight steel fibers, respectively. In addition, by using long steel fibers, fracture energies that were almost 121% and 35% higher were obtained, as compared to those of medium and short steel fibers [3]. This is mainly caused by the fact that using longer steel fibers increases the bonding area between the fiber and the matrix, which leads to a higher fiber pullout load carrying capacity and slip capacity [51]. Additionally, the number of fibers at crack surfaces, which is a major factor that affects the post-cracking tensile behavior, was insignificantly

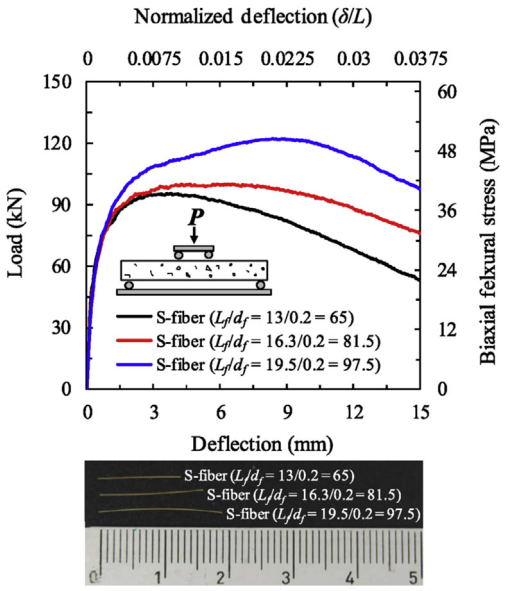

Fig. 12. Biaxial flexural response of UHPFRC panels (placing concrete at the center) [50].

changed by the fiber length at the identical diameter. For instance, the numbers of fibers per unit area were found to be 34.00/cm^2 for short fibers, 33.12/cm^2 for medium fibers, and 35.79/cm^2 for long fibers [3]. The reason for the insignificant change in the number of fibers detected per unit area is that, even though the actual number of fibers included in the mixture decreases with fiber length at an identical volume fraction (because the fibers are included in the mixture based on their volume content), the possibility that fibers will be present at crack surfaces increases with the fiber length.

The post-cracking flexural strength, strength parameters in the tri-linear (or bi-linear) tension-softening curve, and fracture energy were increased almost linearly as the fiber volume fraction increased. Alternatively, the first-cracking flexural strength and the corresponding deflection were insignificantly affected by the fiber volume fraction [31,52,53]. The post-cracking flexural strength of UHPFRC that included short straight steel fibers at the volume fraction of 5% was found to be approximately 64 MPa, which is almost seven times higher than the post-cracking flexural strength without fibers, as shown in Fig. 13 [52]. A higher amount of steel fibers slightly improved the compressive strength and elastic modulus up to a fiber volume fraction of 3% [53]. Since the compressive strength is strongly influenced by the homogeneity of the fiber dispersion, the optimum fiber volume fraction that produces the highest compressive strength is different for different researchers. Prabha et al. [54] reported that UHPFRC with 2 vol% of 13-mm-long straight steel fibers provided the highest compressive strength up to a fiber volume fraction of 3%, whereas Yunsheng et al. [31] reported that the compressive strength continuously increased with an increase in the fiber volume up to 4% (the specimen with 4 vol% of steel fibers exhibited a compressive strength that was 30–50 MPa higher than that without fibers). In addition, the fiber pullout performance was improved by adding up to 2 vol% of the steel fibers into the matrix [53]. By increasing the fiber volume from 1.5 to 2.5%, the tensile strength and strain capacity of UHPFRC were both improved from 8 to 14 MPa and 0.17–0.24% (for straight steel fibers) and from 8 to 15 MPa and 0.33–0.61% (for twisted steel fibers), respectively. However, in the case of hooked-end steel fibers, the tensile strength of UHPFRC increased with increasing fiber volume from 9 to 14 MPa, whereas the strain capacity remained constant at about 0.46% [7].

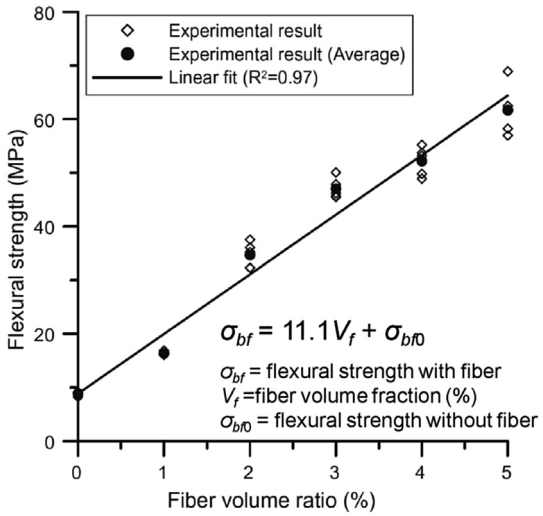

Fig. 13. Relationship between flexural strength and fiber volume fraction [52].

4.4. Effects of fiber orientation

Because of its high fluidity and appropriate viscosity to prevent fiber segregation from the cement matrix, UHPFRC has been used to fabricate structures with various placement methods [55–58]. In accordance with the investigation of Boulekbache et al. [59], fibers are rotated by different flow velocities for flowable fiber-reinforced concrete, as shown in Fig. 14. The fluid exerts forces and moments on the fibers; thus, the fibers are aligned perpendicularly to the flow direction (radial flow in Fig. 14(a)) and parallel to the flow direction (shear flow in Fig. 14(b)). Yang et al. [55] fabricated steel bar-reinforced UHPFRC beams with two different placement methods: (1) placing concrete at one end of the forms and allowing it to flow to the other end and (2) placing concrete at the center and allowing it to flow to both ends. In their test results, the beams where concrete was placed at one end provided the maximum load

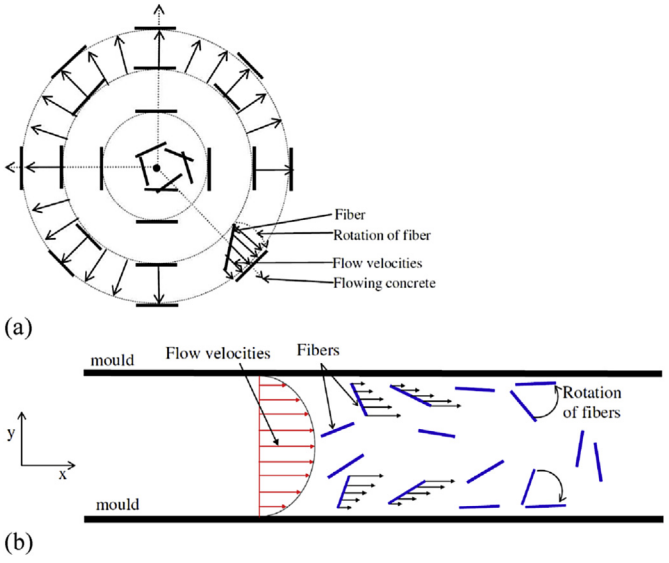

Fig. 14. Schematic view of fiber orientation in (a) fountain (radial) flow, (b) canal channel (shear) flow [59].

that was about 15% higher than when concrete was placed at the center. This is caused by the fact that the flowability of UHPFRC causes more fibers to be oriented in the direction longitudinal to the beam length. Ferrara et al. [56] and Kwon et al. [57] also produced rectangular slabs with different placement methods and investigated the effect of fiber orientation on the flexural performance of UHPFRC. In the case where concrete was placed at one short edge of the mold and allowed to flow [56], the beams (T series) positioned in the vertical direction of the flow direction exhibited poor flexural performance, as compared to the beams (L series) positioned in the parallel direction. This was due to the perpendicular alignment of the fibers to the beam length, as shown in Fig. 15. In the same manner, for the case where concrete was placed at the center (radial flow) [57], the beams located parallel to the flow direction showed much lower load carrying capacities than the beams in other parts. They also exhibited deflection-softening behavior, which is unusual flexural behavior for UHPFRC. From the above observations, it is clear that the fiber orientation characteristics significantly affect the mechanical and structural performance under tension and flexure. Thus, a number of studies [3,4,50,51,56,60–62] have been conducted to quantitatively evaluate how the fiber orientation characteristics influence the mechanical properties of UHPFRC and drew some useful findings.

Wille and Parra-Montesinos [60] investigated the effects of the casting method (layer-casting and middle-casting) and casting speed of a layer-casting method on the flexural behavior of uniaxial UHPFRC beams. They mentioned that by increasing the casting speed, a snake-like flow pattern could be avoided and a thinner layer with a preferred fiber alignment in the beam axis could be obtained; this led to improved flexural performance. In addition, the beams cast in the middle exhibited an intermediate flexural strength value between those of beams cast in layers using a high casting speed and a low casting speed. In a similar way, Yoo et al. [3] reported that beams cast in the middle provided higher flexural strength than those cast in the edge; however, the fracture energy was insignificantly influenced by the casting method because the benefit of the higher strength was offset by a steeper decrease in the post-peak stress. In order to rationally analyze the test results, they also performed image analysis and verified that more steel fibers were located at the middle (at the maximum moment region) for the beams cast in the middle than the beams cast in the edge, as shown in Fig. 16.

Barnett et al. [4] and Yoo et al. [50] investigated the flexural performance of UHPFRC panels under a biaxial stress state. Even though they used different test methods (Barnett et al. [4] used ASTM C 1550 [63] and Yoo et al. [50] used a novel biaxial flexural test (BFT) method suggested by Zi et al. [64]), similar test results

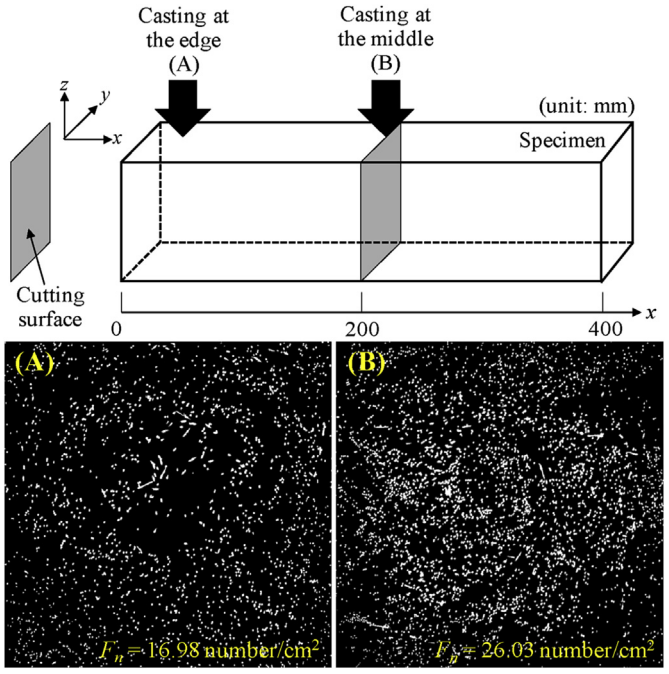

Fig. 16. (a) schematic description of cross-sectional saw cut of UHPFRC beams, (b) transformed binary images obtain at the middle of beams with a size of 100 × 100 × 400 mm³ (using straight steel fibers with a length of 30 mm and a diameter of 0.3 mm) [3].

were obtained. UHPFRC panels cast in the center exhibited significantly higher flexural strengths than panels cast with different placement methods, i.e., casting at several points around the perimeter of the panel, casting randomly, and casting at the one edge. The test results obtained from ASTM C 1550 are shown in Fig. 17. In order to explain their observations, Barnett et al. [4] conducted X-ray computed tomography (CT) analysis. Alternatively, Yoo et al. [50] performed image analysis using binary images at the crack surfaces, which were converted from RGB images obtained with a high-resolution camera. From these analyses, they observed that a greater number of the steel fibers in the panels cast in the center were aligned perpendicular to the flow direction, due to the gradient of the flow velocity, as compared to other panels with different placement methods. This improved fiber alignment resulted in a higher flexural strength and toughness for the panels cast in the center relative to their counterparts.

Kang and Kim [62] numerically analyzed the fiber rotational motion based on Jeffery's equation [65] with the assumption that

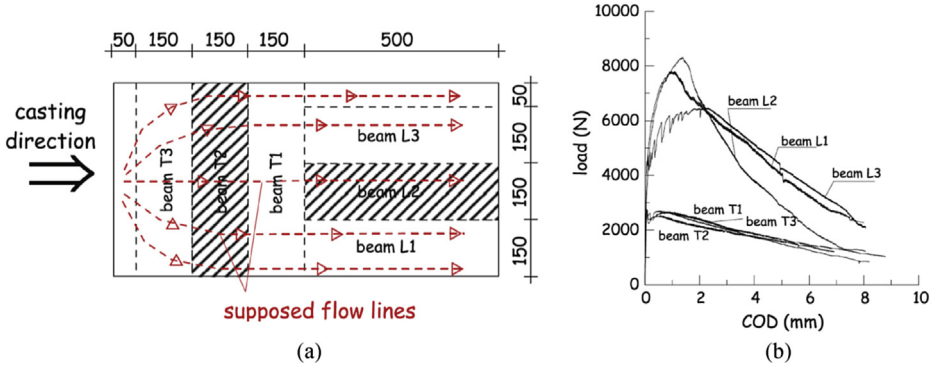

Fig. 15. Effect of fiber orientation on the flexural response; (a) schematic view of slab casting and beam cutting, (b) flexural load-COD curves [56].

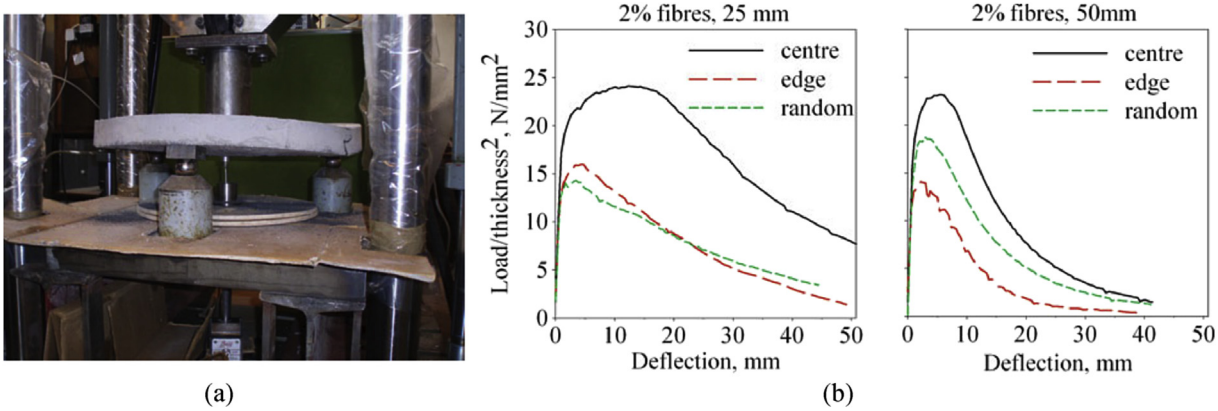

Fig. 17. Round panel tests; (a) picture for test setup (ASTM C 1550), (b) biaxial flexural behaviors [4].

there were no interactions between fibers. They reported that the fibers gradually become more parallel to the flow direction (for shear flow) and more perpendicular to the flow direction (for radial flow) as the flow distance increased. These numerical results are consistent with the actual image analysis results from shear and radial flows that were conducted by Yoo et al. [3,51]. In accordance with Yoo et al. [3] and Lee et al. [66], the probability density function (PDF) of the fiber orientation distributions for both UHPFRC and engineered cementitious composites (ECC), obtained by image analysis, showed totally different behavior from those obtained with the assumptions of two- and three-dimensional (2-D and 3-D) random fiber orientations. However, based on micromechanics-based analysis, it is worth noting that the use of a 2-D random fiber orientation was more advisable for simulating the flexural behavior of uniaxial UHPFRC beams without reinforcing bars than that of a 3-D random fiber orientation [67].

4.5. Size effect

As is already well known, the fracture front of concrete is blunted by micro-cracks at the fracture process zone; this causes unique structural size effects that are different from those predicted by linear elastic fracture mechanics (LEFM) [68]. Most laboratory tests are conducted using a reduced scale; thus, generalizations must be made for larger real structures. Due to this, the size effect in UHPFRC elements has recently been investigated by several researchers [60,69–73]. An et al. [73] analyzed the size effect on the compressive strength of UHPFRC with various fiber dosages. They used cubic specimens of four different sizes (side lengths of 50, 70.7, 100, and 150 mm). It was clear that the larger cubic specimens exhibited lower compressive strengths compared to the smaller samples, as shown in Fig. 18. Specimens without fibers exhibited

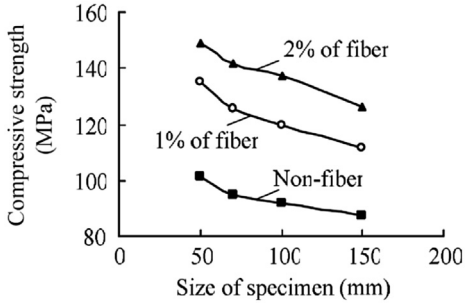

Fig. 18. Compressive strength versus specimen size [73].

similar sensitivity to the size effect on the compressive strength, compared to normal- and high-strength concretes, and as the fiber dosage increased, the size effect became more remarkable. Mahmud et al. [69] and Wille and Parra-Montesinos [60] investigated the size effect on the flexural strength by performing three- and four-point bending tests. From these test results, they concluded that the size effect on the flexural strength of UHPFRC is negligible and follows the yield criterion because of its high ductility. This is consistent with the findings of Spasojavic et al. [74], who stated that the size effect in thin flexural members made of UHPFRC was negligible. Lepech and Li [75] also demonstrated that the ECC showed no significant change in flexural strength according to the specimen size due to its ductile nature. Nguyen et al. [70] also reported that the flexural performance (e.g., flexural strength, normalized deflection, and normalized toughness) of UHPFRC with a higher tensile ductility is less sensitive to the size effect than UHPFRC with a lower ductility. However, their test results were closer to the LEFM criterion than the yield criterion, which was inconsistent with the findings of other previous studies [60,69]. Similarly, Kazemi and Lubell [76] reported that smaller UHPFRC samples had higher compressive strength, first- and post-cracking flexural strengths, and direct shear strengths, compared to larger samples. In particular, an increased size effect on the shear strength was obtained with higher fiber contents. Reineck and Greiner [77] and Frettlöhr et al. [78] also mentioned that the axial tensile and flexural strengths of UHPFRC distinctively decreased with increasing the specimen size (an obvious size effect), and a greater size effect was observed for the flexural strength than for the axial tests [77]. These conflicting results may have been caused by the fact that although the post-cracking flexural behavior is substantially affected by the fiber bridging capacity rather than the matrix strength [67], they did not account for the fiber orientation when the size effect was investigated. Also, the placement methods used for these tests were not clearly described. Therefore, Yoo et al. [72] recently conducted a number of flexural tests of UHPFRC beams with different sizes and performed image analysis to determine the fiber distribution characteristics (i.e., fiber orientation, fiber dispersion, and number of fibers per unit area) at the localized cracks. Similar to the results obtained by Nguyen et al. [70] and Reineck and Greiner [77], the flexural performances of UHPFRC beams, fabricated by placing concrete at one end and allowing it to flow, were noticeably decreased as the specimen size increased (Fig. 19(a)), regardless of the fiber aspect ratio (from 65 to 100) or type (straight and twisted steel fibers). However, the main reason for the size effect in UHPFRC beams was the different fiber distribution characteristics; larger beams led to poor fiber orientation with a lower number of fibers. Yoo et al. [72] ensured that when

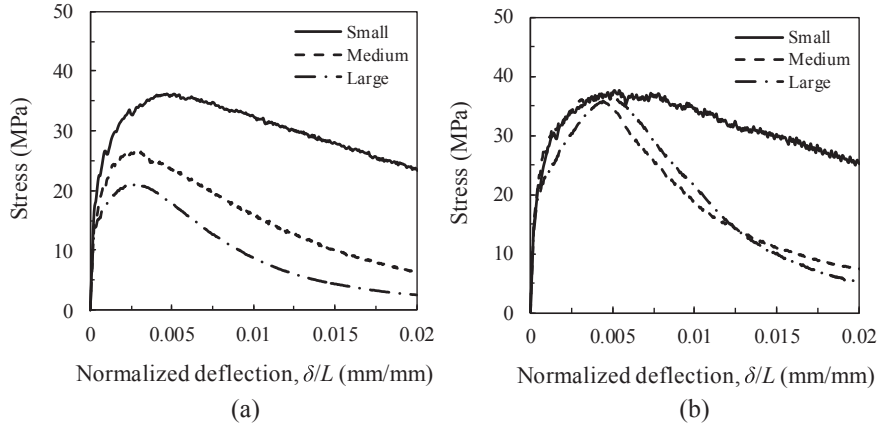

Fig. 19. Size effect on flexural behavior of UHPFRC with; (a) identical placement method, (b) similar fiber distribution characteristics [72].

similar fiber distribution characteristics were obtained for all test beams with different sizes, much less sensitivity to the size effect on the flexural strength was obtained as compared to the case with the different characteristics, as shown in Fig. 19(b). Accordingly, it was concluded that the size effect in UHPFRC beams is mostly due to the different fiber distribution characteristics; thus, by ensuring similar fiber distribution characteristics, an insignificant size effect on the flexural strength can be obtained for UHPFRC containing 2 vol% of steel fibers.

4.6. Loading rate (strain-rate) effects

Because of UHPFRC's excellent mechanical strength and energy absorption capacity based on its unique strain hardening behavior, it has attracted much attention from researchers as a way to enhance the resistance of structure at high rate loadings (e.g., earthquakes, impacts, and blasts). According to a previous study performed by Banthia et al. [11], concrete exhibits a different sensitivity to the strain-rate according to the loading conditions; a minimal sensitivity to the strain-rate was obtained under compression, whereas a maximal sensitivity to the strain-rate was obtained under tension. An intermediate value was observed for flexure. This is caused by the different failure mechanisms under compression and tension; thus, the strain-rate effects of UHPFRC were separately reviewed in this paper according to the loading condition.

4.6.1. For compression

Rong et al. [79] and Lai and Sun [80] investigated the dynamic compressive behavior of UHPFRC with different fiber volume fractions using a split-Hopkinson pressure bar (SHPB). Their test results indicated that the impact resistance was improved by adding more steel fibers, and the compressive strength, strain at the peak (strain capacity), and ultimate strain were noticeably increased with an increase in the strain-rate, as shown in Fig. 20. In addition, they suggested the use of the Johnson_Holmquist_Concrete material model for dynamic compressive simulation of concrete using LS-DYNA and the modified ZWT model (a nonlinear viscoelastic damage model) to describe the constitutive relation of UHPFRC under dynamic loading. A dynamic failure criterion, to predict the maximum strength of UHPFRC, was proposed by Fujikake et al. [81]; this considers the effects of the steel fiber content and strain-rate. By using the dynamic failure criterion, they [81] proposed the following equation to predict the dynamic compressive strength for UHPFRC with 2 vol% of steel fibers.

$$\frac{f'_{cf,d}}{f'_{cf,s}} = \begin{cases} \left(\dfrac{\dot{\varepsilon}}{\dot{\varepsilon}_{sc}}\right)^{0.0055\left[\log\left(\frac{\dot{\varepsilon}}{\dot{\varepsilon}_{sc}}\right)\right]^{0.951}} & (\dot{\varepsilon} \geq \dot{\varepsilon}_{sc}) \\ 1.0 & (\dot{\varepsilon} < \dot{\varepsilon}_{sc}) \end{cases} \quad (5)$$

Here, $f'_{cf,d}$ is the dynamic compressive strength, $f'_{cf,s}$ is the static compressive strength, $\dot{\varepsilon}$ is the strain-rate, and $\dot{\varepsilon}_{sc}$ is the strain-rate corresponding to static compressive loading (1.2×10^{-5}/s).

4.6.2. For tension

Fujikake et al. [82] conducted uniaxial rapid tensile loading tests for prismatic UHPFRC specimens using a commercial mixture of Ductal®. By applying various loading rates from 10^{-4} to 50 m/s (leading to strain-rates from 10^{-6} to 5/s), both the first-cracking and maximum tensile strengths increased as the loading rate increased. However, the initial slope of the stress-elongation relations and the tensile stress-crack opening curves, beyond a crack opening of 2.0 mm, were insignificantly influenced by the loading rate. The tensile strength increased by about 70% as the strain-rate increased from 10^{-6} to 5/s. Fujikake et al. [82] proposed an equation for the dynamic tensile strength of UHPFRC, as follows:

$$f_{tf,d} = f_{tf,s}\left(\frac{\dot{\varepsilon}}{\dot{\varepsilon}_{st}}\right)^{0.0013\left[\log\left(\frac{\dot{\varepsilon}}{\dot{\varepsilon}_{st}}\right)\right]^{1.95}} \quad (6)$$

Here, $f_{tf,d}$ is the dynamic tensile strength, $f_{tf,s}$ is the static tensile strength (10.8 MPa), and $\dot{\varepsilon}_{st}$ is the strain-rate corresponding to static tensile loading (1.0×10^{-6}/s).

Douglas and Billington [83] indicated that post-cracking tensile behavior of ECC is significantly influenced by the specimen geometry; cylindrical ECC specimens showed strain-softening response and a strain capacity that was five times lower than the very thin coupon ECC specimens; this difference in performance was caused by the 3-D random fiber orientations and vertical casting direction. In addition, Toutlemonde et al. [84] pointed out that the fiber volume fraction has an insignificant influence on the strain-rate sensitivity; however, different fiber orientations can result in varied crack development, leading to differences in the dynamic response. Thus, most of the recent studies regarding dynamic tensile tests of UHPFRC have been conducted using a thin (half) dog-bone-shaped specimen, which is able to capture the unique strain-hardening behavior. Wille et al. [85] investigated the tensile behavior of UHPFRC with various steel fiber contents at strain-rates ranging from 10^{-4} to 10^{-1}/s. In their test results, the post-cracking

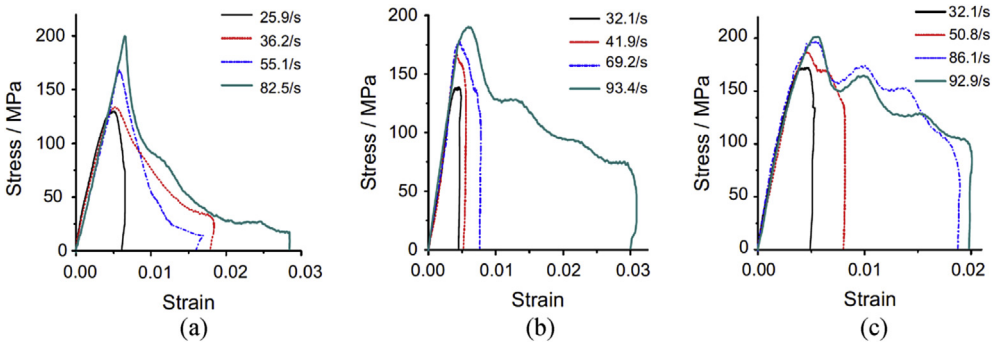

Fig. 20. Dynamic compressive behavior of UHPFRC with; (a) $V_f = 0\%$, (b) $V_f = 3\%$, (c) $V_f = 4\%$ [79].

tensile strength increased by about 20% and the energy absorption capacity increased by about 40% as the strain-rate increased from 10^{-4} to 10^{-1}/s. Tran et al. [86] also experimentally observed that the tensile resistance of UHPFRC was much higher at high strain-rates compared to a static rate. However, although the twisted steel fibers produced the highest tensile resistance at a static rate, the highest impact resistance including the post-cracking strength, strain capacity, and toughness was obtained for UHPFRC with long straight steel fibers. This was caused by the fact that twisted steel fibers broke at high strain-rates while straight steel fibers did not. In the same manner, Wille et al. [87] also reported a lower tensile strength for UHPFRC with twisted steel fibers at higher loading rates compared to those with straight steel fibers; this was caused by the limited strain-rate sensitivity. When using UHPFRC with 2 vol% of twisted fibers, as opposed to 2 vol% of straight fibers, the tensile strength was found to be approximately 10% lower at the strain-rate of 10^{-1}/s. Based on analytical simulation studies, Pyo and El-Tawil [88] proposed a modified strain energy frame impact machine (SEFIM) using a 1.55 m long brass transmitter bar to capture the strain hardening and softening of UHPFRC. Higher strain-rates from 90 to 145/s were achieved relative to those obtained from previous studies [85–87]. Their test results indicated that UHPFRC maintains its strain capacity and has greatly enhanced tensile strength and strain dissipation capacity under increasing strain-rates, as shown in Fig. 21.

4.6.3. *For flexure*

Habel and Gauvreau [89] reported that a significant increase in the flexural strength and fracture energy were obtained for dynamically loaded UHPFRC plates, as compared to samples subjected to quasi-static loading conditions. By performing drop-weight impact tests, Bindiganavile et al. [12] concluded that compact reinforced concrete (CRC), which is a type of UHPFRC with a compressive strength of 200 MPa, exhibited approximately twice strong flexural strength and dissipated three or four times as much energy, compared to those of conventional fiber-reinforced concrete (FRC) with polymeric and steel fibers. This improved performance was caused by the synergistic combined effect of the high strength matrix and the high fiber volume fraction. In addition, CRC was found to be less stress-rate sensitive than conventional FRC, which was similar to the findings of Ross [90] and Yoo et al. [91] who reported that as the strength of concrete increased, a less sensitivity to the strain-rate was obtained under flexure. Yoo et al. [92] also reported that UHPFRC exhibited much higher impact and residual capacities under flexure (strain-rates ranging from 4 to 10/s), as compared to conventional FRCs with compressive strengths ranging from 49 to 180 MPa and 2 vol% of hooked-end steel fibers.

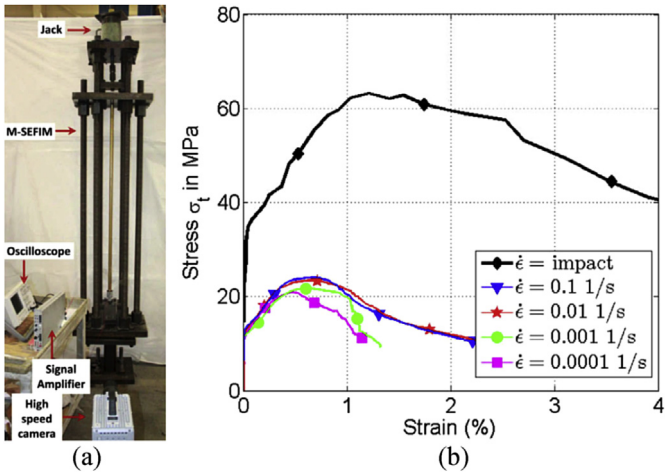

Fig. 21. Impact tensile tests for UHPFRC; (a) test setup, (b) tensile versus strain curves with various strain rates (impact = strain rates ranging from 90 to 145/s) [88].

5. Conclusion

This paper reviewed the state-of-the-art on the mechanical properties of ultra-high-performance fiber-reinforced concrete (UHPFRC). Based on the literature review and discussions, the following conclusions can be drawn:

1) Heat treatment on UHPFRC resulted in acceleration of the hydration process and an increased density, which led to the ultra-high strength. A lower curing temperature generally required a longer curing period to achieve strengths similar to those of heat-treated UHPFRC, i.e., wet curing at 20 °C required 91 days to provide a compressive strength of approximately 200 MPa. In addition, the replacement of fine sand with coarse aggregate with a maximum size of 8 mm has no significant effect on the compressive strength, whereas the flexural strength was decreased.
2) Using silica fume (SF) accelerated the hydration process of UHPFRC, whereas the use of fly ash (FA) and slag delayed the hydration process. Increasing the SF content up to 30% led to an increase in the bond strength and pullout energy. Replacing the SF with FA or slag up to 40% has no significant effect on the compressive strength, whereas using the FA and slag positively affected the flexural strength and toughness. In addition, due to a synergic effect, the combination of 10% rice husk ash (RHA) and 10% SF improved the compressive strength, compared to using only SF.
3) The use of deformed (hooked-end and twisted) steel fibers improved the mechanical properties compared to the

performance of straight steel fibers, i.e., the use of twisted steel fibers increased the tensile strength, strain capacity, and flexural strength by about 32%, 205%, and 167%, respectively, compared to short straight steel fibers. By increasing the length of the straight steel fibers at an identical diameter, higher flexural strength, deflection capacity, toughness, and fracture energy were obtained; this is caused by the better fiber pullout performance without any significant change of the number of fibers at the crack surfaces.

4) The flexural strength of UHPFRC was clearly influenced by the casting method, whereas the fracture energy was not. By increasing the casting speed of the layer-casting method for uniaxial beams, a preferred fiber alignment was observed. This led to the improved flexural performance. The biaxial panels cast in the center had more fibers aligned perpendicular to the crack surfaces; thus, a higher flexural strength was obtained compared to counterpart panels made with other placement methods. Even though the actual probability density function (PDF) for fiber orientation distribution was different to that of 2-D and 3-D random fiber orientations, the assumption of 2-D random fiber orientation was reasonable for simulating the flexural behavior of uniaxial UHPFRC beams without reinforcing bars.
5) Larger UHPFRC samples provided lower mechanical strengths than smaller samples. Additionally, a greater size effect was obtained for the flexural strength than the strengths obtained by axial tests. The size effect on the flexural strength was mainly caused by differences in the fiber distribution characteristics, i.e., larger specimens led to poor fiber orientation and fewer fibers. Thus, an insignificant size effect was obtained for UHPFRC beams with 2 vol% of steel fibers at similar fiber distribution characteristics due to the high ductility.
6) A noticeable increase in the mechanical properties of UHPFRC was obtained at high strain-rates. The tensile strength was increased by approximately 70% by increasing the strain-rate from 10^{-6} to 5/s, and the energy absorption capacity was increased by about 40% by increasing the strain-rate from 10^{-4} to 10^{-1}/s. The fiber volume content has no significant effect on the strain-rate sensitivity. In contrast to the quasi-static loading condition, the use of twisted steel fibers reduced the tensile strength by about 10% compared to straight steel fibers at a high strain-rate of 10^{-1}/s. UHPFRC exhibited approximately twice the strength flexural strength and three or four times higher dissipated energy than conventional fiber-reinforced concrete (FRC).

Based on the review, the following issues are highlighted for further research:

1) There is a conflict between the results from various 'size effect' tests for UHPFRC. These discrepancies are attributed to the size-dependent fiber distribution characteristics. Thus, the fiber distribution characteristics must be addressed when the size effect in UHPFRC is investigated.
2) While it is obvious that twisted steel fibers provided better tensile or flexural performance at a static rate compared to straight steel fibers, the effectiveness of using twisted steel fibers to improve the tensile performance at a high rate loading is still ambiguous. Some researchers have reported that using twisted steel fibers decreases the tensile strength at high rate loading compared to straight steel fibers.
3) Efforts must be made to reduce the production cost of UHPFRC to promote its widespread use. Possible ways are described as follows: (1) replacing cementitious materials or very fine admixtures with coarse aggregate or less expansive mineral admixtures, (2) decreasing the required steel fiber content without noticeably deteriorating the mechanical properties, (3) reducing the amount of superplasticizer, and (4) changing the heat curing process (at 90 °C) to a normal curing process.

Acknowledgments

This research was supported by a grant (16TBIP-C111710-01) from Technology Business Innovation Program funded by Ministry of Land, Infrastructure and Transport of Korean government. Continued support of IC-IMPACTS (Canada India Research Center of Excellence) is also appreciated.

References

[1] AFGC/SETRA, Ultra High Performance Fibre-reinforced Concretes. Interim Recommendations, SETRA, Bagneux, France, 2002, p. 152.
[2] JSCE, Recommendations for Design and Construction of Ultra-high Strength Fiber Reinforced Concrete Structures (Draft), Japan Society of Civil Engineers, Tokyo, Japan, 2004.
[3] D.Y. Yoo, S.T. Kang, Y.S. Yoon, Effect of fiber length and placement method on flexural behavior, tension-softening curve, and fiber distribution characteristics of UHPFRC, Constr. Build. Mater 64 (2014) 67–81.
[4] S.J. Barnett, J.F. Lataste, T. Parry, S.G. Millard, M.N. Soutsos, Assessment of fibre orientation in ultra high performance fibre reinforced concrete and its effect on flexural strength, Mater Struct. 43 (7) (2010) 1009–1023.
[5] S.T. Kang, J.K. Kim, The relation between fiber orientation and tensile behavior in an ultra high performance fiber reinforced cementitious composites (UHPFRCC), Cem. Concr. Res. 41 (10) (2011) 1001–1014.
[6] C.M. Tam, V.W. Tam, K.M. Ng, Assessing drying shrinkage and water permeability of reactive powder concrete produced in Hong Kong, Constr. Build. Mater 26 (1) (2012) 79–89.
[7] K. Wille, D.J. Kim, A.E. Naaman, Strain-hardening UHP-FRC with low fiber contents, Mater Struct. 44 (3) (2011) 583–598.
[8] J. Ma, M. Orgass, F. Dehn, D. Schmidt, N.V. Tue, Comparative investigations on ultra-high performance concrete with and without coarse aggregates, in: Proceedings of the International Symposium on Ultra High Performance Concrete, Kassel, Germany, 2004, pp. 205–212.
[9] K. Wille, A.E. Naaman, G.J. Parra-Montesinos, Ultra-high performance concrete with compressive strength exceeding 150 MPa (22 ksi): a simpler way, ACI Mater J. 108 (1) (2011) 46–54.
[10] D.Y. Yoo, Performance Enhancement of Ultra-high-performance Fiber-reinforced Concrete and Model Development for Practical Utilization, PhD thesis, Korea University, Seoul, South Korea, 2014, p. 586.
[11] N. Banthia, K. Chokri, Y. Ohama, S. Mindess, Fiber-reinforced cement based composites under tensile impact, Adv. Cem. Based Mater 1 (3) (1994) 131–141.
[12] V. Bindiganavile, N. Banthia, B. Aarup, Impact response of ultra-high-strength fiber-reinforced cement composite, ACI Mater J. 99 (6) (2002) 543–548.
[13] M. Yudenfreund, I. Odler, S. Brunauer, Hardened portland cement pastes of low porosity I. Materials and experimental methods, Cem. Concr. Res. 2 (3) (1972) 313–330.
[14] D.M. Roy, G.R. Gouda, A. Bobrowsky, Very high strength cement pastes prepared by hot pressing and other high pressure techniques, Cem. Concr. Res. 2 (3) (1972) 349–366.
[15] H.H. Bache, Densified cement ultra-fine particle-based materials, in: Proceedings of the 2nd International Conference on Superplasticizers in Concrete, Ottawa, 1981, p. 33.
[16] J.D. Birchall, A.J. Howard, K. Kendall, Flexural strength and porosity of cements, Nature 289 (5796) (1981) 388–390.
[17] P. Richard, M. Cheyrezy, Composition of reactive powder concretes, Cem. Concr. Res. 25 (7) (1995) 1501–1511.
[18] C. ASTM, 403. Standard Test Method for Time of Setting of Concrete Mixture by Penetration Resistance. Annual Book of ASTM Standards, ASTM International, West Conshohocken, PA, 2008, p. 7.
[19] D.Y. Yoo, J.J. Park, S.W. Kim, Y.S. Yoon, Early age setting, shrinkage and tensile characteristics of ultra high performance fiber reinforced concrete, Constr. Build. Mater 41 (2013) 427–438.
[20] B.A. Graybeal, Compressive behavior of ultra-high-performance fiber-reinforced concrete, ACI Mater J. 104 (2) (2007) 146–152.
[21] Y. Zhang, W. Zhang, W. She, L. Ma, W. Zhu, Ultrasound monitoring of setting and hardening process of ultra-high performance cementitious materials, NDT E Int. 47 (2012) 177–184.
[22] K. Habel, M. Viviani, E. Denarié, E. Brühwiler, Development of the mechanical properties of an ultra-high performance fiber reinforced concrete (UHPFRC), Cem. Concr. Res. 36 (7) (2006) 1362–1370.
[23] D.Y. Yoo, K.H. Min, J.H. Lee, Y.S. Yoon, Shrinkage and cracking of restrained ultra-high-performance fiber-reinforced concrete slabs at early age, Constr. Build. Mater 73 (2014) 357–365.
[24] J.E. Jonasson, Slipform Construction-calculations for Assessing Protection against Early Freezing, Swedish Cement and Concrete Institute, Stockholm, 1985, pp. 1–13. Fo 4:84.

[25] D.Y. Yoo, J.J. Park, S.W. Kim, Y.S. Yoon, Influence of ring size on the restrained shrinkage behavior of ultra high performance fiber reinforced concrete, Mater Struct. 47 (7) (2014) 1161–1174.
[26] P. Acker, M. Behloul, Ductal® technology: a large spectrum of properties, a wide range of applications, in: Proceedings of the International Symposium on Ultra High Performance Concrete. Germany, 2004, pp. 11–23.
[27] KCI, Design Recommendations for Ultra-high Performance Concrete K-uhpc. KCI-m-12–003, Korea Concrete Institute, Seoul, Korea, 2012.
[28] V. Perry, G. Weiss, Innovative field cast UHPC joints for precast bridge decks – Design, prototype testing and projects, in: Proceedings of the International Workshop on Ultra High Performance Fibre Reinforced Concrete–Designing and Building with UHPFRC: State of the Art Development, Marseille, France, 2009.
[29] E. Brühwiler, E. Denarie, Rehabilitation of concrete structures using ultra-high performance fibre reinforced concrete, in: Proceedings of the 2nd International Symposium on Ultra High Performance Concrete, Kassel, Germany, 2008, pp. 895–902.
[30] K.T. Koh, J.J. Park, G.S. Ryu, S.T. Kang, Effect of the compressive strength of ultra-high strength steel fiber reinforced cementitious composites on curing method, J. Korean Soc. Civ. Eng. 27 (3A) (2007) 427–432.
[31] Z. Yunsheng, S. Wei, L. Sifeng, J. Chujie, L. Jianzhong, Preparation of C200 green reactive powder concrete and its static–dynamic behaviors, Cem. Concr. Compos 30 (9) (2008) 831–838.
[32] J.S. Park, Y.J. Kim, J.R. Cho, S.J. Jeon, Early-age strength of ultra-high performance concrete in various curing conditions, Mater 8 (8) (2015) 5537–5553.
[33] T.M. Ahlborn, D.L. Mission, E.J. Peuse, C.G. Gilbertson, Durability and strength characterization of ultra-high performance concrete under variable curing regimes, in: Proceedings of the 2nd International Symposium on Ultra High Performance Concrete, Kassel, Germany, 2008, pp. 197–204.
[34] A.M. Soliman, M.L. Nehdi, Effect of drying conditions on autogenous shrinkage in ultra-high performance concrete at early-age, Mater Struct. 44 (5) (2011) 879–899.
[35] D.Y. Yoo, S.T. Kang, J.H. Lee, Y.S. Yoon, Effect of shrinkage reducing admixture on tensile and flexural behaviors of UHPFRC considering fiber distribution characteristics, Cem. Concr. Res. 54 (2013) 180–190.
[36] Park SH, Ryu GS, Koh KT, Kim DJ. Effect of shrinkage reducing agent on pullout resistance of high-strength steel fibers embedded in ultra-high-performance concrete. Cem. Concr. Compos;49:59–69.
[37] D.Y. Yoo, J. Kim, G. Zi, Y.S. Yoon, Effect of shrinkage-reducing admixture on biaxial flexural behavior of ultra-high-performance fiber-reinforced concrete, Constr. Build. Mater 89 (2015) 67–75.
[38] D.Y. Yoo, N. Banthia, Y.S. Yoon, Effectiveness of shrinkage-reducing admixture in reducing autogenous shrinkage stress of ultra-high-performance fiber-reinforced concrete, Cem. Concr. Compos 64 (2015) 27–36.
[39] K. Wille, A.E. Naaman, S. El-Tawil, G.J. Parra-Montesinos, Ultra-high performance concrete and fiber reinforced concrete: achieving strength and ductility without heat curing, Mater Struct. 45 (3) (2012) 309–324.
[40] S. Collepardi, L. Coppola, R. Troli, M. Collepardi, Mechanical Properties of Modified Reactive Powder Concrete, 173, ACI Spec Publ, 1997, pp. 1–22.
[41] M. Orgass, Y. Klug, Fibre reinforced ultra-high strength concretes, in: Proceedings of the International Symposium on Ultra High Performance Concrete, Kassel, Germany, 2004, pp. 637–647.
[42] Y.W. Chan, S.H. Chu, Effect of silica fume on steel fiber bond characteristics in reactive powder concrete, Cem. Concr. Res. 4 (7) (2004) 1167–1172.
[43] H. Yazıcı, M.Y. Yardımcı, S. Aydın, A.Ş. Karabulut, Mechanical properties of reactive powder concrete containing mineral admixtures under different curing regimes, Constr. Build. Mater 23 (3) (2009) 1223–1231.
[44] N. Van Tuan, G. Ye, K. Van Breugel, A.L. Fraaij, D. Dai Bui, The study of using rice husk ash to produce ultra high performance concrete, Constr. Build. Mater 25 (4) (2011) 2030–2035.
[45] P. Rougeau, B. Borys, Ultra high performance concrete with ultrafine particles other than silica fume, in: Proceedings of the International Symposium on Ultra High Performance Concrete, Kassel, Germany, 2004, pp. 213–226.
[46] A.E. Naaman, New fiber technology: cement, ceramic and polymeric composites, Concr. Int. 20 (7) (1998) 57–62.
[47] A.E. Naaman, Engineered steel fibers with optimal properties for reinforcement of cement composites, J. Adv. Concr. Tech. 1 (3) (2003) 241–252.
[48] K. Wille, A.E. Naaman, Pullout behavior of high-strength steel fibers embedded in ultra-high-performance concrete, ACI Mater J. 109 (4) (2012) 479–488.
[49] D.Y. Yoo, Y.S. Yoon, Structural performance of ultra-high-performance concrete beams with different steel fibers, Eng. Struct. 102 (2015) 409–423.
[50] D.Y. Yoo, G. Zi, S.T. Kang, Y.S. Yoon, Biaxial flexural behavior of ultra-high-performance fiber-reinforced concrete with different fiber lengths and placement methods, Cem. Concr. Compos 63 (2015) 51–66.
[51] D.Y. Yoo, N. Banthia, G. Zi, Y.S. Yoon, Comparative biaxial flexural behavior of ultra-high-performance fiber-reinforced concrete panels using two different test and placement methods, J. Test. Eval. (2016), http://dx.doi.org/10.1520/JTE20150275 in-press.
[52] S.T. Kang, Y. Lee, Y.D. Park, J.K. Kim, Tensile fracture properties of an ultra high performance fiber reinforced concrete (UHPFRC) with steel fiber, Compos Struct. 92 (1) (2010) 61–71.
[53] D.Y. Yoo, J.H. Lee, Y.S. Yoon, Effect of fiber content on mechanical and fracture properties of ultra high performance fiber reinforced cementitious composites, Compos Struct. 106 (2013) 742–753.
[54] S.L. Prabha, J.K. Dattatreya, M. Neelamegam, M.V. Seshagirirao, Study on stress-strain properties of reactive powder concrete under uniaxial compression, Int. J. Eng. Sci. Technol. 2 (11) (2010) 6408–6416.
[55] I.H. Yang, C. Joh, B.S. Kim, Structural behavior of ultra high performance concrete beams subjected to bending, Eng. Struct. 32 (11) (2010) 3478–3487.
[56] L. Ferrara, N. Ozyurt, M. Di Prisco, High mechanical performance of fibre reinforced cementitious composites: the role of "casting-flow induced" fibre orientation, Mater Struct. 44 (1) (2011) 109–128.
[57] S.H. Kwon, S.T. Kang, B.Y. Lee, J.K. Kim, The variation of flow-dependent tensile behavior in radial flow dominant placing of Ultra High Performance Fiber Reinforced Cementitious Composites (UHPFRCC), Constr. Build. Mater 33 (2012) 109–121.
[58] D.Y. Yoo, N. Banthia, S.T. Kang, Y.S. Yoon, Effect of fiber orientation on the rate dependent flexural behavior of ultra-high-performance fiber-reinforced concrete, Compos Struct. (2016) (under review).
[59] B. Boulekbache, M. Hamrat, M. Chemrouk, S. Amziane, Flowability of fibre-reinforced concrete and its effect on the mechanical properties of the material, Constr. Build. Mater 24 (9) (2010) 1664–1671.
[60] K. Wille, G.J. Parra-Montesinos, Effect of beam size, casting method, and support conditions on flexural behavior of ultra-high-performance fiber-reinforced concrete, ACI Mater J. 109 (3) (2012) 379–388.
[61] S.T. Kang, B.Y. Lee, J.K. Kim, Y.Y. Kim, The effect of fibre distribution characteristics on the flexural strength of steel fibre-reinforced ultra high strength concrete, Constr. Build. Mater 25 (5) (2011) 2450–2457.
[62] S.T. Kang, J.K. Kim, Numerical simulation of the variation of fiber orientation distribution during flow molding of Ultra High Performance Cementitious Composites (UHPCC), Cem. Concr. Compos 34 (2) (2012) 208–217.
[63] C. ASTM, 1550-12a. Standard Test Method for Flexural Toughness of Fiber-reinforced Concrete (Using Centrally Loaded Round Panel), Annual Book of ASTM Standards, ASTM International, West Conshohocken, PA, 2012, p. 14.
[64] G. Zi, H. Oh, S.K. Park, A novel indirect tensile test method to measure the biaxial tensile strength of concretes and other quasibrittle materials, Cem. Concr. Res. 38 (6) (2008) 751–756.
[65] G.B. Jeffery, The motion of ellipsoidal particles immersed in a viscous fluid, Proc. Roy. Soc. Lond. 102 (715) (1922) 161–179.
[66] B.Y. Lee, J.K. Kim, Y.Y. Kim, Prediction of ECC tensile stress–strain curves based on modified fiber bridging relations considering fiber distribution characteristics, Comput. Concr. 7 (5) (2010) 455–468.
[67] D.Y. Yoo, S.T. Kang, N. Banthia, Y.S. Yoon, Nonlinear finite element analysis of ultra-high-performance fiber-reinforced concrete beams, Int. J. Damage Mech. (2016), http://dx.doi.org/10.1177/1056789951561255 9 in-press.
[68] Z.P. Bažant, Size effect in blunt fracture: concrete, rock, metal, J. Eng. Mech. 110 (4) (1984) 518–535.
[69] G.H. Mahmud, Z. Yang, A.M. Hassan, Experimental and numerical studies of size effects of ultra high performance steel fibre reinforced concrete (UHPFRC) beams, Constr. Build. Mater 48 (2013) 1027–1034.
[70] D.L. Nguyen, D.J. Kim, G.S. Ryu, K.T. Koh, Size effect on flexural behavior of ultra-high-performance hybrid fiber-reinforced concrete, Compos Part B Eng. 45 (1) (2013) 1104–1116.
[71] D.L. Nguyen, G.S. Ryu, K.T. Koh, D.J. Kim, Size and geometry dependent tensile behavior of ultra-high-performance fiber-reinforced concrete, Compos Part B Eng. 58 (2014) 279–292.
[72] D.Y. Yoo, N. Banthia, S.T. Kang, Y.S. Yoon, Size effect in ultra-high-performance concrete beams, Eng. Frac Mech. 157 (2016) 86–106.
[73] M.Z. An, L.J. Zhang, Q.X. Yi, Size effect on compressive strength of reactive powder concrete, J. Chin. Univ. Min. Technol. 18 (2) (2008) 279–282.
[74] A. Spasojavic, D. ReDaelli, M. Fernandez Ruiz, A. Muttoni, Influence of tensile properties of UHPFRC on size effect in bending, in: Proceedings of the 2nd International Symposium on Ultra High Performance Concrete. Kassel, Germany, 2008, pp. 303–310.
[75] M. Lepech, V.C. Li, Brittle Matrix Composites-7, Warsaw, Poland, in: Preliminary Findings on Size Effect in ECC Structural Members in Flexural, 2003, pp. 57–66.
[76] S. Kazemi, A.S. Lubell, Influence of specimen size and fiber content on mechanical properties of ultra-high-performance fiber-reinforced concrete, ACI Mater J. 109 (6) (2012) 675–684.
[77] K.H. Reineck, S. Greiner, Scale Effect and Combined Loading of Thin UHPFRC Members. Advances in Construction Materials, 2007, pp. 211–218.
[78] B. Frettlöhr, K.H. Reineck, H.W. Reinhardt, Size and shape effect of UHPFRC prisms tested under axial tension and bending, in: Proceedings of High Performance Fiber Reinforced Cement Composites 6, Netherlands, 2012, pp. 365–372.
[79] Z. Rong, W. Sun, Y. Zhang, Dynamic compression behavior of ultra-high performance cement based composites, Int. J. Impact Eng. 37 (5) (2010) 515–520.
[80] J. Lai, W. Sun, Dynamic behaviour and visco-elastic damage model of ultra-high performance cementitious composite, Cem. Concr. Res. 39 (11) (2009) 1044–1051.
[81] K. Fujikake, K. Uebayashi, T. Ohno, Y. Shimoyama, M. Katagiri, Dynamic properties of steel fiber reinforced mortar under high-rates of loadings and triaxial stress states, in: Proceedings of the 7th International Conference on Structures under Shock and Impact, Montreal, 2008, pp. 437–446.
[82] K. Fujikake, T. Senga, N. Ueda, T. Ohno, M. Katagiri, Effects of strain rate on tensile behavior of reactive powder concrete, J. Adv. Concr. Tech. 4 (1) (2006) 79–84.
[83] K.S. Douglas, S.L. Billington, Strain rate dependence of HPFRCC cylinders in

monotonic tension, Mater Struct. 44 (1) (2011) 391–404.
[84] F. Toutlemonde, C. Boulay, J. Sercombe, F. Le Maou, R. Adeline, Characterization of reactive powder concrete (RPC) in direct tension at medium to high loading rates, in: Proceedings of the 2nd International Conference on Concrete under Severe Conditions: Environment and Loading, Vol. II, CONSEC'98, Tronso, Norway, 1998, 1998, pp. 887–896.
[85] K. Wille, S. El-Tawil, A.E. Naaman, Strain rate dependent tensile behavior of ultra-high performance fiber reinforced concrete, in: Proceedings of High Performance Fiber Reinforced Cement Composites 6. Netherlands, 2012, pp. 381–387.
[86] N.T. Tran, T.K. Tran, D.J. Kim, High rate response of ultra-high-performance fiber-reinforced concretes under direct tension, Cem. Concr. Res. 69 (2015) 72–87.
[87] K. Wille, M. Xu, S. El-Tawil, A.E. Naaman, Dynamic impact factors of strain hardening UHP-FRC under direct tensile loading at low strain rates, Mater Struct. 49 (4) (2016) 1351–1365.
[88] S. Pyo, S. El-Tawil, Capturing the strain hardening and softening responses of cementitious composites subjected to impact loading, Constr. Build. Mater 81 (2015) 276–283.
[89] K. Habel, P. Gauvreau, Response of ultra-high performance fiber reinforced concrete (UHPFRC) to impact and static loading, Cem. Concr. Compos 30 (10) (2008) 938–946.
[90] C.A. Ross, Review of strain rate effects in materials, in: Proceedings: Structures under Extreme Loading Conditions, ASME Pressure Vessels and Piping, Orlando, 1997, pp. 255–262.
[91] D.Y. Yoo, Y.S. Yoon, N. Banthia, Flexural response of steel-fiber-reinforced concrete beams: effects of strength, fiber content, and strain-rate, Cem. Concr. Compos 64 (2015) 84–92.
[92] D.Y. Yoo, N. Banthia, Y.S. Yoon, Ultra high performance fiber reinforced concrete under impact loading, in: Proceedings of the 7th RILEM Workshop on High Performance Fiber Reinforced Cement Composites (HPFRCC-7), Stuttgart, Germany, 2015, pp. 217–224.